International Journal of Applied Pharmaceutics

ISSN- 0975-7058 Vol 16, Issue 2, 2024

Original Article

FORMULATION, ANALYSIS AND VALIDATION OF NANOSUSPENSIONS-LOADED VORICONAZOLE TO ENHANCE SOLUBILITY

SARMAD AL-EDRESI[1*], MAZIN THAMIR ABDUL-HASAN[2], YASMIEN ABDUL HADI SALAL[3]

Department of Pharmaceutics and Industrial Pharmacy, Faculty of Pharmacy, University of Kufa, Najaf-52001, Iraq
[*]Corresponding author: Sarmad Al-Edresi; [*]Email: s.aledresi@uokufa.edu.iq

Received: 11 Oct 2023, Revised and Accepted: 28 Dec 2023

ABSTRACT

Objective: This study aimed to enhance the solubility of voriconazole (VRZ) *via* loading to nanosuspensions using solvent/anti-solvent technique. The optimisation of independent variables (polymer concentrations) was carried out to achieve the desired particle size and maximise the percentage of entrapment efficiency (EE %) and drug loading (DL %) using design-expert®software.

Methods: Design-Expert® software, version 13, was used to design and optimise nanosuspensions-loaded VRZ using 2^3 factorial designs. Concentrations of polyvinylpyrrolidone, hydroxypropyl methylcellulose and poloxamers were selected as independent variables to achieve ideal particle size, polydispersity index (PDI), entrapment efficacy (EE %) and drug loading (DL %). Atomic force microscopy (AFM), differential scanning calorimetry (DSC) and saturated solubility were used to assess the lyophilized nanoparticles. The compatibility between the drug and the polymers was studied using Fourier transform infrared spectroscopy (FTIR).

Results: The particle size, PDI, EE %, and DL % were in the range of 15.6–145.6 nm, 0.010-0.120, 55.9 %-91.9 %, and 6.68-36.76 %, respectively. The saturated solubility of nanosuspensions-loaded VRZ (NS-VRZ) relative to free VRZ was increased tenfold in DW and twelvefold in PBS (pH 7.4). DSC thermogram confirmed the incorporation of VRZ in the nanosuspensions. The AFM of NS-VRZ validated spherical tiny particle size with a smooth surface. There is no chemical interaction between VRZ and the polymers, according to an FTIR investigation.

Conclusion: The solubility of VRZ was successfully enhanced by loading to nanosuspensions. The solvent/anti-solvent technique was proven to be cost-effective, easy to operate and suitable for the preparation of NS-VRZ using Design-Expert®software.

Keywords: Design-expert® software, Voriconazole, Solvent/anti-solvent technique, Nanosuspensions

DOI: https://dx.doi.org/10.22159/ijap.2024v16i2.49591 Journal homepage: https://innovareacademics.in/journals/index.php/ijap

INTRODUCTION

Drug solubility in aqueous media is an important consideration to address early in the drug discovery process. Approximately 40 % of novel chemical entities generated in the pharmaceutical sector are nearly water-insoluble [1]. The biopharmaceutics classification system divides drugs into four categories: class I (very soluble and permeable), class II (highly permeable but poorly soluble), class III (highly soluble but weakly permeable), and class IV (poorly soluble and poorly permeable) [2]. The II and IV classes are typically characterized by high molecular weights, significant log P values and poor water solubility. Pharmaceutical nanosuspensions are aqueous dispersions of insoluble drug particles that are nanosized and stabilized by surfactants. Nanoparticles, on the other hand, are drug carriers that are either polymeric or lipid colloidal [3-5]. When a drug molecule has several limitations, such as the inability to form salt, high molecular weight, dose, log P and melting point, nanosuspension is the only choice accessible [6]. The inherent nature of molecular complexation employing cyclodextrin in pharmaceutical formulations to increase the formulation volume due to the large molecular weight of the complexing agent is a key restriction. By keeping active pharmaceutical ingredients in a crystalline condition while allowing for increased drug loading during formulation development, nanosuspensions can tackle such unique drug delivery difficulties [7]. Because of the reduced usage of toxic, non-aqueous solvents and extreme pH, accommodating large drug amounts with minimal dose volume provides significant benefits in parenteral and ophthalmic drug delivery systems [8]. Other benefits include enhanced stability, extended drug release, increased efficacy through tissue targeting, minimal first-pass metabolism and deep lung deposits [9]. These benefits have accelerated the development of nanosuspension technology in recent decades. Despite the difficulties of production, choosing the right unit operation, equipment and process optimization can help to mitigate these issues [10].

The VRZ, a lipophilic drug, is a second-generation novel triazole derivative of fluconazole with excellent broad-spectrum activity that is commercially accessible for oral and intravenous administration [11]. It belongs to class II in the BCS, which is characterized by low solubility and high permeability. The VRZ is very effective against fluconazole-resistant *Candida* species, such as *Candida krusei*, *Candida glabrata*, and *Candida albicans* [12]. It has fungicidal *in vitro* action against all *Aspergillus* species, moulds including *Scedosporium* species and *Fusarium* species associated with *keratitis* [13].

This study aimed to enhance the solubility of VRZ *via* loading to nanosuspensions using a solvent/anti-solvent technique.

MATERIALS AND METHODS

Material

The VRZ powder was purchased from Srini (India), hydroxypropyl methylcellulose (HPMC E5) and poloxamers (PXM-188) from Hyperchem (China). The disodium hydrogen phosphate (Na_2HPO_4), potassium dihydrogen phosphate (KH_2PO_4), sodium chloride (NaCl), polyvinylpyrrolidone (PVP K-30) and ethanol were obtained from CDH (India), Himdia (India), LAD (India) Alpha chemical (India) and HaymanKimia (UK), respectively.

Method

Experimental design

A 2^3-factorial design was selected using Design-Expert® software to determine the appropriate concentrations of HPMC E5, PVP K-30 and PXM 188 needed to create nanosuspensions with the best possible responses. The concentrations of A (PVP K-30), B (HPMC

E5), and C (PXM 188) were chosen as independent variables, while R1 (particle size) and R2 (PDI), R3 (EE %), and R4 (DL %) were chosen as dependent variables [14]. In this design, three criteria were assessed at three levels of concentrations-lower (25 mg), middle (112.5 mg), and higher (200 mg), each with the corresponding codes being-1, 0 and+1, respectively.

The design resulted in 9 runs, as listed in table 1.

Table 1: The 2^3factorial design of NS-VRZ using design-expert® software

Run	A	B	C
1	+1	-1	+1
2	-1	-1	-1
3	-1	+1	-1
4	-1	+1	-1
5	-1	-1	+1
6	+1	+1	-1
7	+1	-1	+1
8	-1	-1	-1
9	-1	+1	+1

Preparation of nanosuspension-loaded VRZ

The NS-VRZ were prepared by solvent-evaporation technique. The VRZ powder was dissolved in 2 ml of ethanol (solvent) to create the drug solution, which was then injected at a rate of 1 ml per minute into 20 ml of DW (anti-solvent) containing several stabiliser combinations in various concentrations (A, B and C). Thereafter, the prepared nanosuspensions were ultra-sonicated for 20 min in a bath sonicator. Solid nanoparticles started to precipitate immediately. The nanosuspensions were placed later in a magnetic stirrer and allowed for an hour to allow the organic solvent to evaporate. Finally, the optimum nanosuspension was lyophilized using a Labconco freeze drier (USA).

Characterization of nanoparticles

Particle size analysis

Using the ABT-9000 Nano Laser particle size analyser, particle size parameters were determined. At a constant temperature of 25 °C and a scattering angle of 90° [15]. The particle size (R1) and PDI (R2) of the prepared nanosuspensions were measured. The sample that has a low polydispersity index mean monodisperse, while the high-level mean wide-speared particle distribution. The normal level of PDI values is 0-0.05, which means monodisperse standard, 0.05-0.08 refers to nearly monodisperse, 0.08-0.7 indicates mid-range PDI and more than 0.7 means very polydisperse [14, 16].

Determination of entrapment efficiency and drug loading

The dialysis membrane was used to assess the entrapment efficiency and drug loading [17]. A 1 ml sample was placed in the dialysis membrane, which was then dialyzed for 12 h against 100 ml of phosphate buffer saline solution (PBS, pH 7.4). After appropriate dilution, the amount of VRZ in the dialysis membrane (entrapped) was measured at 256 nm against PBS buffer as a blank. By dividing the amount of entrapped drug by the total amount of drug utilized, it is possible to determine the entrapment efficiency of VRZ [18, 19].

Development and evaluation of the optimized formulation

The Design-Expert® software suggested an optimal formula based on maximizing drug loading and entrapment efficiency and minimizing particle size and polydispersity index. The optimum formula was selected using the desirability index, which has a value between 0 and 1, and examines the desirable range for each response. These criteria were established, and the best formula was chosen [4, 20].

Freeze-drying of nanosuspension

The lyophilisation (freeze drying) is one of the most effective methods used for the solidification of the nanosuspension by water removal *via* sublimation and desorption under a high vacuum [21]. The water removal was conducted through freeze-drying to get the nanoparticles of VRZ in the dried powder state from the prepared nanosuspensions. The formulation was pre-frozen at-30 °C for 12 h then lyophilized utilizing a vacuum freeze dryer at a pump operating at a pressure of (0.46 mbar) and the controlled temperature of (-40 °C) for 72 h [22].

Characterization of lyophilized powder

Determination of the saturated solubility

The saturated solubility of pure VRZ and VRZ-NPs was determined in different media of DW, and PBS (pH 7.4). An excess amount of the compound was added to a test tube with 10 ml of each media. Each tube was sealed in aluminium foil and placed in a water bath shaker for 48 h at 37 °C The sample was taken and filtered using a 0.45 µm filter syringe and absorbance was determined by spectrophotometer. The concentration was then, calculated from the corresponding calibration curve [23].

Atomic force microscope (AFM)

The AFM is used to precisely quantify the particle size of nanoparticles while under controlled environmental conditions by scanning surfaces. A small amount of the sample was applied to freshly cleaved mica. Particle size, histogram of particle size distribution and 3D surface morphology of NS-VRZ were obtained [24].

Differential scanning calorimetry (DSC)

The DSC is used to evaluate the compatibility between VRZ and other additives and to evaluate the drug's crystalline form, particularly when incorporated into nanoparticles [25]. The thermal characteristics of the pure VRZ, A (PVP K30), B (HPMC E5), C (PXM 188) and NS-VRZ were examined by an automatic thermal analyser system [26].

Drug-excipients compatibility studies

These studies were achieved to identify any sign of interaction or complexation which may happen between VRZ and stabilizers used in the preparation of the nanoparticles.

Fourier Transform Infrared Spectroscopy (FTIR) study

Different FTIR spectra were obtained with FTIR for pure VRZ, A (PVP K30), B (HPMC E5), C (PXM 188), P-NPs (polymers nanoparticles without drug) and NS-VRZ. The potassium bromide was crushed up and added to all of these samples. The resulting spectra ranged from 4000 to 400 cm^{-1} in wave number [27].

RESULTS AND DISCUSSION

Particle size and polydispersity index analysis

The particle size results were ranged from 15.6 nm–145.6 nm. Other formulas' sizes are within this range. These variations in particle size could be associated with variations in the affinities and concentrations of polymer molecules for drug particles [28]. The formula showed the highest particle size value was (Run 8), while the smallest was (Run 9) as illustrated in table 2. This could be due to a high stabilizers ratio in (Run 9), which decreases surface tension and stabilises the newly formed surfaces during

the precipitation process, resulting in a nanosuspension with smaller particles [29]. The stabiliser molecules wrapped the drug particle surface properly [30].

Results of the PDI ranged from (0.010-0.120) for (Run 9) and (Run 3), respectively (table 2). Run 9 showed monodispersed PDI, while (Run 3) showed a mid-range of PDI [31, 32].

Table 2: The 2^3 factorial design responses parameters of VRZ nanosuspension formulations.

Run	R1	R2	R3	R4
1	44.3	0.055	90.5	9.53
2	107.1	0.045	91.9	36.76
3	125.3	0.120	80.2	13.37
4	115.4	0.055	55.9	9.32
5	19.9	0.015	57.8	9.63
6	118.8	0.032	57.6	6.06
7	49.3	0.046	63.5	6.68
8	145.6	0.058	91.5	36.62
9	15.6	0.010	78.7	8.28

Determination of drug entrapment efficiency and drug loading of nanosuspension

The highest percentage of the drug entrapment efficiency for the prepared formulations was 91.9% (Run 2), while the lowest percentage of the drug entrapment efficiency was 55.9% (Run 4) as listed in table 2. This could be due to a high HPMC E5 concentration in (Run2) that increases the viscosity of the internal phase, which reduces the migration of the drug, leading to an increase in the entrapped amount of VRZ [33].

The drug loading results ranged from 6.68 to 36.76 % as listed in table 2. These results revealed that the drug loading was increased with the increase of polymer concentrations and entrapment efficiency % and this was consistent with the finding of Dora and his colleagues (2010), who found that an increase in the polymer ratio and EE %, increased the DL % [34].

Statistical analysis

The obtained data were fitted into different models and a best-fit model was suggested by the Design-Expert® software depending on parameters such as p-value, adjusted determination coefficient (adj. R2), and predicted determination coefficient (pred. R2). A p-value of (ABC) was 0.0029, 0.0498 and<0.0001 (i.e., ≤ 0.05) for R1, R2 and R4, respectively. This indicates that the model is significant and the three polymers have a significant effect on these responses. The ratio for R1, R2 and R4 was 6.1325, 5.2792 and 18.0553, respectively. This indicates an adequate signal. The best-fit model equations generated for R1, R2 and R4 were shown in Equation 1, 2 and 3.

R1=+65.34-43.65A-10.29B+0.3125C…….. E. q. 1

R2=+0.049-0.0214A-0.0051B+0.0069C+0.0011AB+0.0059AC-0.0151BC+0.0091ABC…….. E. q. 2

R4=+12.06-3.98A-4.41B-4.55C+2.35AB+3.12AC+3.40BC-2.49ABC. . E. q. 3

For R1, the average coefficient of the linear model was 65.34 and the coefficient for individual PVP K-30, HPMC E5 and PXM 188 were 43.65, 10.29 and 0.3125, respectively. The negative charge in the equation indicates that PVP K-30 and HPMC E5 had a negative effect on particle size, but the PVP K-30 had a higher negative effect on particle size, while PXM 188 had a positive effect on particle size. This confirmed that the effect of PVP K-30 concentration on nanoparticle size was more than HPMC E5 and PXM 188 as shown in Equation 1. These results agreed with the results of Mandlik and Ranpise (2017) [35], who found that the effect of chitosan concentration on nanoparticle size was more pronounced than STPP depending on the coefficient values for chitosan and STPP were 229.50 and 99.67, respectively.

For R2, the average coefficient of the factorial model was 0.049 and the coefficient for individual PVP K-30, HPMC E5 and PXM 188 were 0.0214, 0.0051 and 0.0069, respectively. The PVP K-30 and HPMC E5 had a negative effect on PDI. The PVP K-30 had a higher negative effect, while PXM 188 had a positive effect on PDI. This indicated that the effect of PVP K-30 concentration on particle size distribution was more pronounced than HPMC E5 and PXM 188 as shown in Equation 2.

For R4, the average coefficient of the factorial model was 12.06 and the coefficient for individual PVP K-30, HPMC E5 and PXM 188 were 3.98, 4.41 and 4.55, respectively. The PVP K-30, HPMC E5 and PXM 188 had a negative effect on DL %. This indicates that when polymer concentrations increased, the DL% decreased. For EE % (R3), the model F-value was high in all models that imply, so the model is not significant. P-values of (ABC) were more than 0.05 indicating that the model is not significant because no one of the model terms exceeds the t-value limit.

Optimization and evaluation of the prepared formulations

The optimized formula was developed based on the statistical evaluations of Design-Expert® software that suggest several combinations as an optimum formula. The optimized formula combination includes PVP K-30 (150 mg), HPMC E5 (180 mg) and PXM-188 (82 mg). The optimum formula was prepared and characterised later. The predicted values of particle size, PDI, EE and DL were 72.56 nm, 0.049, 73.34 % and 12.04 %, respectively. On the other hand, experimental results were 64.65 nm, 0.059, 86.73 % and 10.17% for particle size, PDI, EE and DL, respectively. The relative error between the predicted values and experimental values of each response was calculated in Equation 4.

$$\text{Relative error} = \frac{(\text{predicted} - \text{experimental})}{\text{predicted}} \text{…… E. q. 4}$$

The relative error for particle size, PDI, EE % and DL % was 0.1, 0.2, 0.18 and 0.16. Low values of the relative error showed a reasonable agreement between predicted values and experimental values. This demonstrated the model's viability and ascertained the effects of polymers on the particle size, PDI, entrapment efficiency and drug loading [36].

Determination of saturation solubility

The saturated solubility of pure VRZ was measured in different media. The drug has poor water solubility was 26.73±1 µg. ml^{-1}, however, the solubility was lower in basic media, 10.8±0.7 µg. ml^{-1}, due to weak basicity nature of the drug (pKa = 1.76) [37]. The NS-VRZ solubility was increased eightfold in DW; while in PBS (pH 7.4) has increased by elevenfold. The breaking of the drug microparticles' perfect structure into nanoparticles is an explanation for the solubility improvement [38]. In contrast to the crystalline state of pure VRZ, nanoparticles' amorphous structure results in a high energy of interfacial tension that increases its solubility [39].

Atomic force microscope (AFM)

The morphological analysis and particle size of NS-VRZ performed by AFM revealed regular to spherical-shaped nanoparticles with a size of (35.6 nm) and approved by the histogram of particle size distribution as seen in fig. 1. In contrast, the particle size estimated by the ABT-9000 particle size analyser was 61.35 nm. The particle size of the optimized NS-VRZ obtained by AFM was smaller than that measured by the ABT-9000 particle size analyser and this difference because a particle size analyser could, only, provide data on the volumetric mean diameter of a large number of particles; it is challenging to get findings that reflect actual size distribution.

Fourier transform infrared spectroscopy (FTIR)

The FTIR study was carried out for pure VRZ, PVP K30, HPMC E5, PXM 188, nanosuspensions-free VRZ and NS-VRZ as shown in fig. 2. The FTIR spectrum of Pure VRZ showed O-H stretching at 3425.58 cm^{-1}, C-N aryl stretching at 1346.31 cm^{-1} and C-F stretching band at 1498–1425.4 cm^{-1}, C-H alkane at 2891.30 cm^{-1}. For the stabilizers, PVP k30 showed a strong absorbance band at 1676.14 cm^{-1} due to the C=O of tertiary amide and at 2956.87 cm^{-1} due to C-H stretching. A very broad band was shown at 3464.15 cm^{-1} due to O-H stretching vibrations of absorbed water. This broadband was confirmed by the broad endothermic peak detected in the DSC experiments. Wegiel and his colleagues (2014) highlighted similar FTIR peaks of PVP K-30 [40]. For HPMC E5, the characteristic peaks were shown at 3400 cm^{-1} due to O-H stretching vibration peak, 1153.43 cm^{-1} due to C-O-C stretching vibration peak and 1109.07 cm^{-1} due to C-O stretching. Oh and his colleagues (2012) highlighted similar FT-IR peaks of HPMC E5 [41].

The FTIR spectrum of PXM 188 was characterized by principal absorption peaks at 2887.44 cm^{-1} due to aliphatic C-H stretching, as shown in fig. 2. As well as the O-H bending that appeared at 1354.03 cm^{-1} and C-O stretching appeared at 1111 cm^{-1}. These results were also consistent with the results published by Sharma *et al.* (2013) [42]. The FTIR results of VRZ nanoparticles showed the presence of the main peaks of pure VRZ that appeared at 3408.22 cm^{-1}, 1336.67 cm^{-1}, 1498-1429.25 cm^{-1} and 2883.58 cm^{-1} for O-H stretching, C-N aryl stretching, C-F stretching and C-H alkane, respectively (fig. 2). The FTIR peaks of polymers nanoparticles showed at 3435.22 cm^{-1}, 2347.37 cm^{-1}, 1645.26 $cm^{-1}$and 1093.64 $cm^{-1}$for PVP K-30 and HPMC E5 (O-H stretching), PXM 188 (O-H bending), PVP K-30 (C=O of tertiary amide), and HPMC E5 and PXM 188 (C-O stretching). As a result of the finding of polymer nanoparticles and NS-VRZ, there was no significant shift in the FTIR spectrum, indicating no interaction or complexation between the drug and polymers during the preparation of NS-VRZ [15].

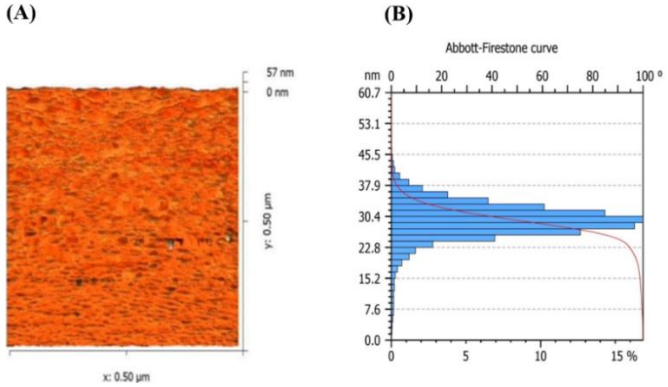

Fig. 1: AFM images. (A) 2D AFM image of NS-VRZ and (B) Histogram of particle size distribution of NS-VRZ

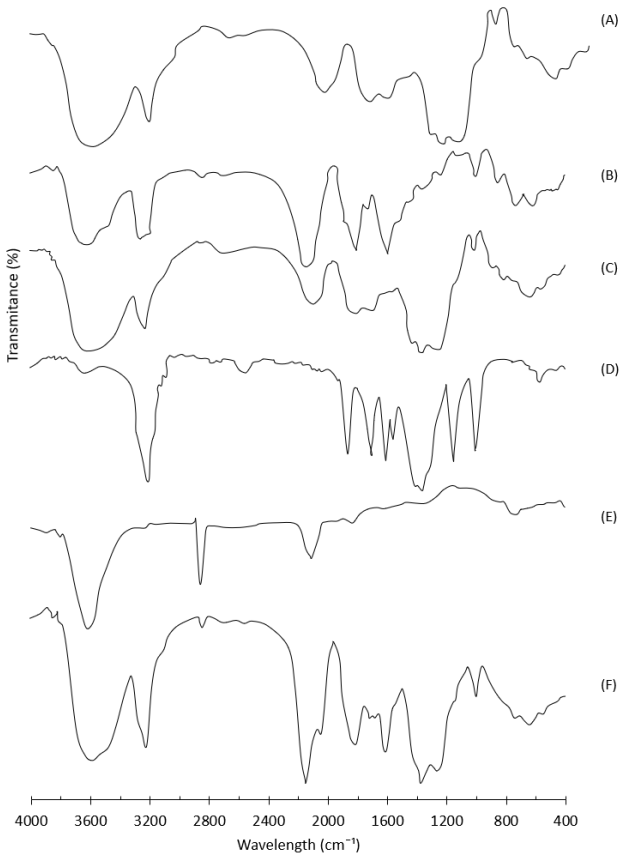

Fig. 2: FTIR images (A) pure VRZ compound; (B) PVP K-30 polymer; (C) HPMC E5 polymer; (D) PXM 188 polymer; € Nanosuspensions-free VRZ; and (F) NS-VRZ

Differential scanning calorimetry (DSC)

The DSC thermogram of pure VRZ showed a sharp exothermic peak at 135.89 °C as shown in fig. 3. The DSC of PVP K-30 showed a broad endotherm at 114.89 °C, as seen in fig. 2. This broad endotherm indicated that water was lost due to the extremely hygroscopic nature of the PVP polymer [43]. The DSC thermogram of HPMC E5 showed a broad endothermic peak in the range of 101.42 °C, which might be attributed to the dehydration of water molecules. NOVIzA and HALIM, (2017) [44] reported a similar peak of HPMC E5.

In general, the DSC thermogram of PXM 188 revealed a broad endotherm at 62.64 °C. The DSC thermogram of NS-VRZ showed the complete disappearance of VRZ melting point, giving a strong indication that the drug lost the crystallinity state and converted to an amorphous form.

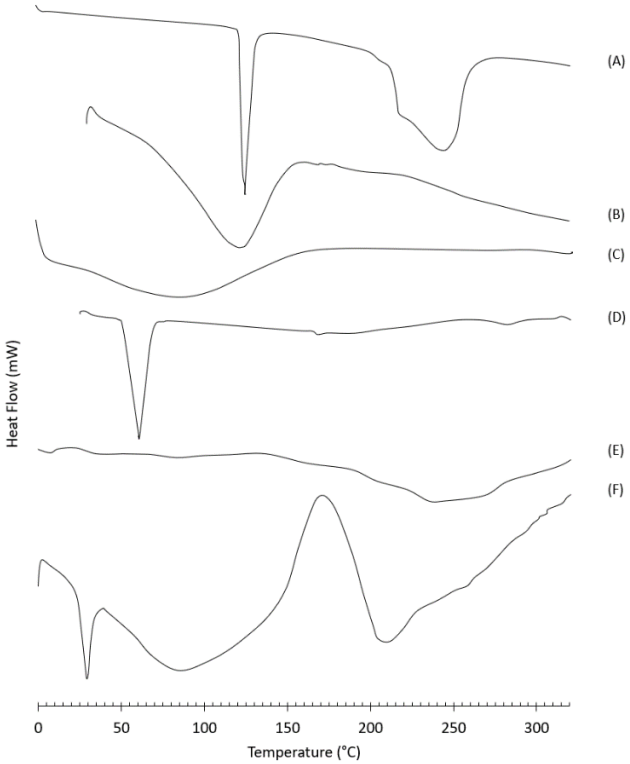

Fig. 3: DSC thermogram of (A) pure VRZ; (B) PVP K-30; (C) HPMS E5; (D) PXM 188 (E) Nanosuspensions-free VRZ (F) NS-VRZ

CONCLUSION

The NS-VRZ were successfully prepared using different combinations of stabilizers such as PVP K-30, HPMC E-5 and PXR 188 in various concentrations. The solvent-antisolvent method was considered as an effective way to increase the saturation solubility of VRZ and its dissolution rate, and it is cost-effective and easy to operate. The optimum formula exhibited a decreased particle size and stabilised drug particles. The FTIR and DSC studies revealed no chemical interaction between VRZ and the stabilizers used in the preparation of nanosuspension. Surface morphology of drug nanoparticles, visualized by AFM, illustrated spherical-shaped NS-VRZ with a smooth surface and accurate particle size was obtained comparable to that obtained by particle size analyser.

FUNDING

Nil

AUTHORS CONTRIBUTIONS

All authors are contributed equally.

CONFLICT OF INTERESTS

Declared none

REFERENCES

1. Chen L, Wang Y, Zhang J, Hao L, Guo H, Lou H. Bexarotene nanocrystal-oral and parenteral formulation development, characterization and pharmacokinetic evaluation. Eur J Pharm Biopharm. 2014;87(1):160-9. doi: 10.1016/j.ejpb.2013.12.005, PMID 24333772.
2. Bonthagarala B, Lakshmi Sai PD, K VS, G AK, Rao BN, Dasari V. Enhancement of dissolution rate of clofibrate BCS Class–II drug by using liquisolid compact technology. Int J Biomed Adv Res 2015;6(3):228. doi: 10.7439/ijbar.v6i3.1891.
3. Edis Z, Wang J, Waqas MK, Ijaz M, Ijaz M. Nanocarriers-mediated drug delivery systems for anticancer agents: an overview and perspectives. Int J Nanomedicine. 2021;16:1313-30. doi: 10.2147/IJN.S289443, PMID 33628022.
4. AlEdresi SS, Alshaibani AJ, Abood AN. Enhancing the loading capacity of kojic acid dipalmitate in liposomes. Lat Am J Pharm. 2020;39(7):1-7.
5. Albo Hamrah KTK, Al-Shaibani AJN, Al-Edresi SS, Al-Gburi KMH. AA comparative study of quality control testing on candesartan cilexetil conventional tablets in iraq. Int J App Pharm. 2020;12(2):103-8. doi: 10.22159/ijap.2020v12i2.36220.
6. Bhakay A, Rahman M, Dave RN, Bilgili E. Bioavailability enhancement of poorly water-soluble drugs via nanocomposites: formulation processing aspects and challenges. Pharmaceutics. 2018;10(3):1-62. doi: 10.3390/pharmaceutics10030086, PMID 29986543.
7. Aledresi SS, Abdulrazza IF, Alshaibani AJ. Enhancing the solubility of nimesulide by loading to a nanoemulsion. Lat Am J Pharm. 2020;39(11):2299-308.
8. Al-Hamadani MH, Al-Edresi S. Formulation and characterization of hydrogel of proniosomes loaded diclofenac sodium. Int J Drug Deliv Technol. 2022;12(1):132-6. doi: 10.25258/ijddt.12.1.24.
9. Kumar M, Jha A, Dr M, Mishra B. Targeted drug nanocrystals for pulmonary delivery: a potential strategy for lung cancer therapy. Expert Opin Drug Deliv. 2020;17(10):1459-72. doi: 10.1080/17425247.2020.1798401, PMID 32684002.

10. Jacob S, Nair AB. Cyclodextrin complexes: perspective from drug delivery and formulation. Drug Dev Res. 2018;79(5):201-17. doi: 10.1002/ddr.21452, PMID 30188584.
11. Mohan WS, B BK, K RN. A review on biological activity of 1, 3-diazole derivatives. Int J Curr Pharm Sci 2022;14(5):1-3. doi: 10.22159/ijcpr.2022v14i5.2030.
12. Sharifzadeh A, Shokri H, Katiraee F. Anti-adherence and anti-fungal abilities of *thymol* and *carvacrol* against *candida* species isolated from patients with oral *candidiasis* in comparison with fluconazole and voriconazole. Jundishapur J Nat Pharm Prod. 2021;16(1):1-7. doi: 10.5812/jjnpp.65005.
13. Walther G, Zimmermann A, Theuersbacher J, Kaerger K, Von lilienfeld-toal M, Roth M. Eye infections caused by filamentous fungi: spectrum and antifungal susceptibility of the prevailing agents in germany. J Fungi (Basel). 2021;7(7):1-14. doi: 10.3390/jof7070511, PMID 34206899.
14. Alhagiesa AW, Ghareeb MM. The formulation and characterization of nimodipine nanoparticles for the enhancement of solubility and dissolution rate. Iraqi J Pharm Sci. 2021;30(2):143-52.
15. El-Emam GA, Girgis GNS, El-Sokkary MMA, El-Azeem Soliman OA, Abd El Gawad AEGH. Ocular inserts of voriconazole-loaded proniosomal gels: formulation, evaluation and microbiological studies. Int J Nanomedicine. 2020;15:7825-40. doi: 10.2147/IJN.S268208, PMID 33116503.
16. Satyajit C, Rao MB, Patro CN, Swain S, Taria S, Kumar S. Formulation, characterization and *in vitro* evaluation for solubility enhancement of a poorly water-soluble drug using nanoedge technique. World J Pharm Res. 2014;3:2152-67.
17. Hao YM, Li K. Entrapment and release difference resulting from hydrogen bonding interactions in niosome. Int J Pharm. 2011;403(1-2):245-53. doi: 10.1016/j.ijpharm.2010.10.027, PMID 20971171.
18. Huang T, Wang Y, Shen Y, Ao H, Guo Y, Han M. Preparation of high drug-loading celastrol nanosuspensions and their anti-breast cancer activities *in vitro* and *in vivo*. Sci Rep. 2020;10(1):8851. doi: 10.1038/s41598-020-65773-9, PMID 32483248.
19. Abdalla KF, Kamoun EA, El Maghraby GM. Optimization of the entrapment efficiency and release of ambroxol hydrochloride alginate beads. J App Pharm Sci. 2015;5(4):13-9. doi: 10.7324/JAPS.2015.50403.
20. Madan JR, Adokar BR, Dua K. Development and evaluation of *in situ* gel of pregabalin. Int J Pharm Investig. 2015;5(4):226-33. doi: 10.4103/2230-973X.167686, PMID 26682193.
21. Powar TA, Hajare AA. Lyophilized ethinylestradiol nanosuspension: fabrication, characterization and evaluation of *in vitro* anticancer and pharmacokinetic study. Indian J Pharm Sci. 2020;82(1):54-9. doi: 10.36468/pharmaceutical-sciences.622.
22. Fonte P, Reis S, Sarmento B. Facts and evidences on the lyophilization of polymeric nanoparticles for drug delivery. J Control Release. 2016;225:75-86. doi: 10.1016/j.jconrel.2016.01.034, PMID 26805517.
23. Patil M, Waydande S, Pawar P. Design and evaluation of topical solid dispersion composite of voriconazole for the treatment of ocular *keratitis*. Ther Deliv. 2019;10(8):481-92. doi: 10.4155/tde-2019-0021, PMID 31462154.
24. Dolenc A, Govedarica B, Dreu R, Kocbek P, Srcic S, Kristl J. Nanosized particles of orlistat with enhanced *in vitro* dissolution rate and lipase inhibition. Int J Pharm. 2010;396(1-2):149-55. doi: 10.1016/j.ijpharm.2010.06.003, PMID 20540997.
25. Jassim ZE, Hussein AA. Formulation and evaluation of clopidogrel tablet incorporating drug nanoparticles. Int J Pharm Sci. 2014;6(1):838-51.
26. Rizal S, Abdullah CK, Olaiya NG, Sri Aprilia NA, Zein I, Surya I. Preparation of palm oil ash nanoparticles: Taguchi optimization method by particle size distribution and morphological studies. Appl Sci. 2020;10(3):1-15. doi: 10.3390/app10030985.
27. Ahmed TA, Aljaeid BM. A potential in situ gel formulation loaded with novel fabricated poly(lactide-co-glycolide) nanoparticles for enhancing and sustaining the ophthalmic delivery of ketoconazole. Int J Nanomedicine. 2017;12:1863-75. doi: 10.2147/IJN.S131850, PMID 28331311.
28. Liu P, Viitala T, Kartal Hodzic A, Liang H, Laaksonen T, Hirvonen J. Interaction studies between indomethacin nanocrystals and peo/ppo copolymer stabilizers. Pharm Res. 2015;32(2):628-39. doi: 10.1007/s11095-014-1491-3, PMID 25145336.
29. Prasetyo J, Sulaiman TNS, Lukitaningsih E. Synthesis, characterization, and optimization of biodegradable pcl-peg-pcl triblock copolimeric micelles as nanocarriers for hydrophobic drug solubility enhancer. Int J Curr Pharm Sci. 2020;12(2):6-10. doi: 10.22159/ijcpr.2020v12i2.37478.
30. Van Eerdenbrugh B, Vermant J, Martens JA, Froyen L, Van Humbeeck J, Augustijns P. A screening study of surface stabilization during the production of drug nanocrystals. J Pharm Sci. 2009;98(6):2091-103. doi: 10.1002/jps.21563, PMID 18803265.
31. Abbas HK, Wais FMH, Abood AN. Preparation and evaluation of ketoprofen nanosuspension using solvent evaporation technique. Iraqi J Pharm Sci. 2017;26(2):41-55. doi: 10.31351/vol26iss2pp41-55.
32. Gadad AP, P SC, PMD, Mastiholimath VS. Moxifloxacin loaded polymeric nanoparticles for sustained ocular drug delivery. PCI- Approved-IJPSN 2018;5(2):1727-34. doi: 10.37285/ijpsn.2012.5.2.8.
33. Sharma M, Kohli S, Dinda A. *In vitro* and *in vivo* evaluation of repaglinide loaded floating microspheres prepared from different viscosity grades of HPMC polymer. Saudi Pharm J. 2015;23(6):675-82. doi: 10.1016/j.jsps.2015.02.013, PMID 26702263.
34. Dora CP, Singh SK, Kumar S, Datusalia AK, Deep A. Development and characterization of nanoparticles of glibenclamide by solvent displacement method. Acta Pol Pharm. 2010;67(3):283-90. PMID 20524431.
35. Mandlik SK, Ranpise NS. Implementation of experimental design methodology in preparation and characterization of zolmitriptan-loaded chitosan nanoparticles. Int Curr Pharm J. 2017;6(3):16-22. doi: 10.3329/icpj.v6i3.32684.
36. Rane Y, Mashru R, Sankalia M, Sankalia J. Effect of hydrophilic swellable polymers on dissolution enhancement of carbamazepine solid dispersions studied using response surface methodology. AAPS PharmSciTech. 2007;8(2):27. doi: 10.1208/pt0802027, PMID 17622105.
37. Vanstraelen K, Maertens J, Augustijns P, Lagrou K, de Loor H, Mols R. Investigation of saliva as an alternative to plasma monitoring of voriconazole. Clin Pharmacokinet. 2015;54(11):1151-60. doi: 10.1007/s40262-015-0269-z, PMID 25910879.
38. Lakshmi P, Kumar GA. Nanosuspension technology: a review. Int J Pharm Sci. 2010;2(4):35-40.
39. Muller RH, Peters K. Nanosuspensions for the formulation of poorly soluble drugs: I. International Journal of Pharmaceutics. 1998;160(2):229-37. doi: 10.1016/S0378-5173(97)00311-6.
40. Wegiel LA, Mauer LJ, Edgar KJ, Taylor LS. Mid-infrared spectroscopy as a polymer selection tool for formulating amorphous solid dispersions. J Pharm Pharmacol. 2014;66(2):244-55. doi: 10.1111/jphp.12079, PMID 24433425.
41. Oh MJ, Shim JB, Yoo H, Lee GY, Jo H, Jeong SM. The dissolution property of raloxifene hcl solid dispersion using hydroxypropyl methylcellulose. Macromol Res. 2012;20(8):835-41. doi: 10.1007/s13233-012-0127-x.
42. Sharma A, Jain CP, Tanwar YS. Preparation and characterization of solid dispersions of carvedilol with poloxamer 188. J Chil Chem Soc. 2013;58(1):1553-7. doi: 10.4067/S0717-97072013000100012.
43. Sethia S, Squillante E. Solid dispersion of carbamazepine in pvp k30 by conventional solvent evaporation and supercritical methods. Int J Pharm. 2004;272(1-2):1-10. doi: 10.1016/j.ijpharm.2003.11.025, PMID 15019063.
44. Zaini E, Fitriani L, Effendy S, Noviza D, Halim A. Preparation and characterization of solid dispersion telmisartan-hydroxypropyl methyl cellulose (HPMC) E5 LV by co-grinding method. Orient J Chem. 2017;33(2):873-8. doi: 10.13005/ojc/330236.